SOFT GROUND IMPROVEMENT VIA VERTICAL DRAINS AND VACUUM ASSISTED PRELOADING

Buddhima Indraratna*

Professor and Head, School of Civil, Mining and Environmental Engineering, Director, Centre for Geomechanics and Railway Engineering; University of Wollongong, Wollongong City, NSW 2522, Australia

Cholachat Rujikiatkamjorn

Senior Lecturer, School of Civil, Mining and Environmental Engineering, University of Wollongong, NSW 2522, Australia

A. S. (Bala) Balasubramaniam

Professor of Geotechnical Engineering, Griffith University, Gold Coast, Queensland, Australia

Geoffrey McIntosh

Principal, Douglas Partners Pty Ltd, Unanderra, NSW Australia

*Author for correspondence:

Prof. B. Indraratna

Faculty of Engineering

University of Wollongong

Wollongong, NSW 2522

Australia.

Ph: +61 2 4221 3046

Fax: +61 2 4221 3238

SOFT GROUND IMPROVEMENT VIA VERTICAL DRAINS AND VACUUM ASSISTED PRELOADING

Buddhima Indraratna, Cholachat Rujikiatkamjorn, A. S. (Bala) Balasubramaniam, and Geoffrey McIntosh

ABSTRACT

Application of vacuum assisted preloading is an imperative method when a considerable load is required to meet the desired rate of settlement and an increase in the undrained shear strength upon consolidation. Moreover, where lateral displacements at the edge of a coastal embankment need to be controlled, application of vacuum pressure with a cut off offers the optimum solution. To facilitate vacuum propagation, vertical drains are usually employed in conjunction. The installation of vertical drains using a steel mandrel creates significant remoulding of the subsoil surrounding the drains thereby, reducing soil permeability and adversely affecting the soil consolidation process. In this paper, the simulation of vacuum assisted consolidation using the spectral method and finite element analysis is carried out. Subsequently, the 2D and 3D numerical multi-drain analyses are conducted to predict the excess pore pressures, lateral and vertical displacements. The performance of two selected case histories at the sites of Suvarnabhumi Airport, Thailand and Tianjin Port, China are discussed and analysed. The numerical predictions are then compared with the available field data. Finally, a procedure for the design of vertical drains is presented with a worked-out example.

INTRODUCTION

Soft clay deposits possess a low bearing capacity and high compressibility characteristics. Therefore, it is imperative to apply ground improvement techniques to the existing soft soils prior to construction, in order to prevent unacceptable differential settlement. The application of prefabricated vertical drains (PVDs) and preloading (surcharge and vacuum load) has become one of the most viable soil improvement techniques. Vertical drains provide considerably shortened horizontal drainage paths for pore water flow, thereby accelerating the soil consolidation (Hansbo, 1981; Indraratna and Redana, 2000; Bergado et al. 2002; Chai et al. 2010). In order to control the risk of embankment failure, surcharge embankments with vacuum application are usually employed to accelerate the rate of settlement without increasing the excess pore pressure (Qian et al., 1992; Shang et al., 1998; Chu et al. 2000, Saowapakpiboon et al. 2010). This practice has been employed for land reclamation and port projects as a high surcharge embankment over the soft dredged fills cannot be raised due to various stability issues (Chu and Yan, 2005). The PVD system facilitates the vacuum pressure distribution to deep subsoil layers in the absence of the surcharge load influence, thereby increasing the consolidation rate (Chu et al. 2006, Leong et al. 2010). The vacuum system enhances the stability of any raised embankment by minimizing the excess pore pressure at its base, and increasing the shear strength of the sand platform. Vacuum consolidation with PVDs is a sustainable option as it does not leave any chemical residue in the soil or groundwater, and has no unacceptable noise levels compared to driven piles. Moreover, vacuum consolidation is isotropic, thereby minimizing the excessive lateral displacement due to high surcharge.

In this paper, modified radial consolidation theory using the spectral method capturing the variation of soil permeability with depth is proposed. The equivalent (transformed) plane

strain conversion employing the modified Cam-clay theory was compared with the actual three-dimensional finite element analysis. It has been shown that 2D plane strain finite element analysis is often adequate to predict settlements, pore pressures and lateral displacements if the conversion from axissymmetry to plane strain ensures the same time consolidation response. Two case histories are discussed and analysed, including the Suvarnabhumi Airport (Thailand) and Tianjin Port in China. The predictions are compared with the available field data.

THEORETICAL MODELLING FOR SOFT GROUND CONSOLIDATION VIA VERTICAL DRAINS AND VACUUM PRELOADING: A SINGLE DRAIN ANALYSIS

The vacuum consolidation theory for radial drainage with smear effect was proposed by Mohamedelhassan and Shang, (2002) and Indraratna et al. (2005a). Recently, Rujikiatkamjorn and Indraratna (2009) a proposed comprehensive solution to vacuum-assisted consolidation with both vertical and horizontal drainage including the smear effect, applicable to a single layer soil. Walker and Indraratna (2009) proposed a rigorous solution via spectral method for multi-layer soil improved by vacuum and surcharge preloading via PVDs.

In a unit cell (Fig. 1), the average pore pressure $\bar{u}$ at normalized depth Z is given by:

$$\frac{m_v}{\overline{m}_v}\frac{\partial \bar{u}}{\partial t} = -\left[dT_h\frac{\eta}{\overline{\eta}}\bar{u} - dT_v\left(\frac{\partial}{\partial Z}\left(\frac{k_v}{\overline{k}_v}\right)\frac{\partial \bar{u}}{\partial Z} + \frac{k_v}{\overline{k}_v}\frac{\partial^2 \bar{u}}{\partial Z^2}\right)\right] + f(Z,t) \tag{1}$$

$$dT_v = \frac{\overline{c}_v}{H^2} \tag{2}$$

$$dT_h = \frac{2\overline{\eta}}{\gamma_w \overline{m}_v} \tag{3}$$

$$\overline{c}_v = \frac{\overline{k}_v}{\gamma_w \overline{m}_v} \tag{4}$$

$$Z = \frac{z}{H} \tag{5}$$

$$f(Z,t) = \frac{m_v}{\overline{m}_v}\frac{\partial \overline{\sigma}}{\partial t} + dT_h \frac{\eta}{\overline{\eta}} w \tag{6}$$

where, r_e = drain influence radius, γ_w = unit weight of water, μ = dimensionless parameter influenced by smear zone, k_h = horizontal soil permeability $\overline{k}_v$ = initial vertical soil permeability, H = soil thickness, k_v =horizontal soil permeability, $\overline{m}_v$ = initial coefficient soil volume compressibility, m_v = coefficient soil volume compressibility, $\overline{\sigma}$ = average total stress, t =time, w =pore pressure at the soil drain boundary.

For constant permeability in the smear zone (Fig. 2a) the value of μ can be determined from (Hansbo 1981):

$$\mu = \ln(n/s) + (\kappa)\ln(s) - 0.75 \tag{7}$$

For linear variation of permeability in the smear zone (Fig. 2b), μ can be determined from (Walker and Indraratna 2006):

$$\mu_L = \ln\left(\frac{n}{s}\right) - \frac{3}{4} + \frac{\kappa\,(s-1)}{s-\kappa}\ln\left(\frac{s}{\kappa}\right) \tag{8}$$

For parabolically varying smear zone (Fig. 2c), the μ parameter can be determined from (Walker and Indraratna 2007):

5

$$\mu = \ln\left(\frac{n}{s}\right) - \frac{3}{4} + \frac{\kappa(s-1)^2}{(s^2 - 2\kappa s + \kappa)}\ln\left(\frac{s}{\sqrt{\kappa}}\right) - \frac{s(s-1)\sqrt{\kappa(\kappa-1)}}{2(s^2 - 2\kappa s + \kappa)}\ln\left(\frac{\sqrt{\kappa} + \sqrt{\kappa-1}}{\sqrt{\kappa} - \sqrt{\kappa-1}}\right) \tag{9}$$

where, $n = r_e/r_w$ and $s = r_s/r_w$, and κ is the ratio of undisturbed horizontal permeability to smear zone permeability at the drain/soil interface.

The average excess pore pressure at depth Z, time t, can be expressed by:

$$\bar{u}(Z,t) = \int_0^\tau \int_0^1 \bar{u}_\delta(Z,t,\zeta,\tau)f(Z,t)\,d\zeta\,d\tau \tag{10}$$

Based on the spectral method, Eq. 10 can be expressed in matrix form as:

$$\bar{u}(Z,t) \approx \mathbf{\Phi v E}(\mathbf{\Gamma v})^{-1}[\theta_1 \quad \theta_2 \quad \dots \quad \theta_N]^T \tag{11}$$

The diagonal matrix $\mathbf{E}$ can be represented by:

$$\mathbf{E}(t) = \mathrm{diag}[\exp(-\lambda_1 t) \quad \exp(-\lambda_2 t) \quad \cdots \quad \exp(-\lambda_N t)] \tag{12}$$

where, λ is an Eigen value of matrix $\mathbf{\Gamma}^{-1}\mathbf{\Psi}$. The eigenvector associated with each Eigen value makes up the columns matrix $\mathbf{v}$ (i.e. v_{i1} is the eigenvector associated with λ_1). $\mathbf{\theta}$ is a column vector defined by:

$$\theta_i = 2(1 - \cos(M_i))/M_i \tag{13}$$

To determine the average pore pressure between depth Z_1 and Z_2 the $\phi_j(Z)$ terms in $\mathbf{\Phi}$ are replaced with:

$$\bar{\phi}_j(Z_1, Z_2) = (\cos(M_j Z_1) - \cos(M_j Z_2))/M_j(Z_2 - Z_1) \tag{14}$$

The above method is straight forward in determining the average pore pressure values within a soil layer, across some layers, or across all layers. The spectral method is a meshless

approach producing a series solution to the consolidation problem based on matrix operations. Equation (11) shows that the soil consolidation can be reduced to a series of matrix operations.

Application to a case history

The Suvarnabhumi Airport is located about 30km east of Bangkok, Thailand. At this site, soft estuarine clay deposits often present considerable construction problems because of low bearing capacity and high compressibility (Seah 2006). Appropriate ground improvement techniques to prevent excessive settlement and lateral movement are required prior to commencement of the construction of permanent structures. In the past, the site was used mainly for aqua-cultural and agricultural activities. The area is often flooded during the wet season and therefore the moisture content of soil is generally very high throughout the year.

The subsoil profile can be divided into five distinctive layers. A weathered crust of approximately 2m thickness (highly overconsolidated clay) overlies a very soft to medium clay, which extends beyond 10m below the ground surface. Beneath the medium clay layer, a light-brown stiff clay layer is found within a depth range depth of 10-21m. The ground-water level varies between 0.5 and 1.5m below the surface. The typical soil profile and its properties are illustrated in Fig. 3. The moisture content of the very soft clay layer changes from 75 to 105%, while in the lower parts of the layer (10-14m) it varies from 45 to 75%. The plastic limit and liquid limit of the upper and lower layers are comparable, in the range of 85 to 105% and 15 to 45%, respectively (Fig. 3).

As reported by Bergado et al. (1998), at this site, two embankments were built with PVDs (100 mm × 3 mm) installed at 1m spacing in a triangular pattern. PVDs of 15m in length were installed under the Embankment TV1, and 12m long PVDs were installed beneath the Embankment TV2. Soil parameters are tabulated in Table 1. A 60 kPa suction

pressure was applied and the embankment height was subsequently raised to a height of 2.5 m (γ =18 kN/m^3). The calculated and measured surface settlements for the two embankments based on the spectral analysis, along with the surcharge and assumed vacuum loading stages, are illustrated in Fig. 4. Loss of vacuum may be attributed to air leaks along drain length and surface. The calculated surface settlements agree well with the measured values verifying the capability of the proposed model to analyse multi-layer problems with different loading stages.

THEORETICAL MODELLING FOR SOFT GROUND CONSOLIDATION VIA VERTICAL DRAINS AND VACUUM PRELOADING: MULTI-DRAIN ANALYSIS

A unit cell theory for vacuum consolidation including a single drain assuming equal strain was proposed by Indraratna et al. (2005a). The obvious constraint of this single drain analysis is that it cannot successfully predict the overall consolidation in a large project where an array of drains is installed. Essentially, a single drain analysis can only be applicable at the embankment centerline where the lateral displacements are negligible. Towards the embankment toe, the analysis using a single drain approach can be quite inaccurate mainly due to the non-equal surcharge load distribution, large lateral strain conditions, effects of embankment geometry and heave at the embankment toe (Indraratna and Redana, 1997 Indraratna et al., 2005a).

To analyse the multi-drain problem using a plane strain finite element analysis, the appropriate equivalence conversion must be established to obtain the same time-settlement curves. Hird et al. (1992) proposed an equivalent plane strain technique, which can be used in numerical modeling. Realistic field predictions require the in-situ properties to be converted to equivalent 2D plane strain properties, especially with regard to the permeability

coefficients, vacuum pressure and drain geometry (Indraratna et al. 2005, Tran and Mitachi 2006). Chai et al. (2001) proposed an approximate method for analyzing PVD improved subsoils, whereby an equivalent vertical hydraulic conductivity was derived to conveniently combine the effect of vertical and horizontal hydraulic conductivities of the natural subsoil. However, this technique cannot be used to simulate the propagation of vacuum pressure. The permeability conversion for equivalent plane strain condition has been considered as a simple but accurate approach as the drain and smear zone geometry remains the same. Below is a summary of the conversion from the true axisymmetric condition to the equivalent plane strain model by Indraratna et al. (2005a).

The corresponding ratio of the smear zone permeability to the undisturbed zone permeability in plane strain analysis ($\frac{k_{s,ps}}{k_{h,ps}}$) can be obtained by:

$$\frac{k_{s,ps}}{k_{h,ps}} = \frac{\beta}{\frac{k_{h,ps}}{k_{h,ax}}\left[\ln\left(\frac{n}{s}\right) + \frac{k_{h,ax}}{k_{s,ax}}\ln(s) - \frac{3}{4}\right] - \alpha} \tag{15}$$

$$\beta = \frac{2(s-1)}{n^2(n-1)}\left[n(n-s-1) + \frac{1}{3}(s^2 + s + 1)\right] \tag{16}$$

$$\alpha = \frac{2}{3}\frac{(n-s)^3}{n^2(n-1)} \tag{17}$$

$$s = d_s/d_w \tag{18}$$

$$n = d_e/d_w \tag{19}$$

where, $k_{s,ax}$ and $k_{h,ax}$ = lateral soil permeability in the smear zone and in the undisturbed zone, respectively, in the axisymmetric condition. d_e = the diameter of soil influence zone, d_s = the smear zone diameter, d_w = the equivalent PVDs diameter.

The undisturbed lateral permeability ratio of equivalent plane strain to axisymmetric permeability can be determined by:

$$\frac{k_{h,ps}}{k_{h,ax}} = \frac{0.67\,(n-1)^2\big/n^2}{[\ln(n) - 0.75]} \qquad (20)$$

An equivalent vacuum pressure can now be expressed by:

$$p_{0,ps} = p_{0,ax} \qquad (21)$$

Case Study of Tianjin Ports: Site descriptions, soil parameters and embankment characteristics

Due to the rapid development of the Tianjin Port, a new pier was required to be constructed on reclamation land for a new storage facility. At this site, clay slurry dredged from the seabed has been used to form the top 3-4m of the soil deposit. The thickness of soft muddy clay below the reclaimed soil was approximately 5m, followed by a 7.5m thick soft clay layer. A 6m thick stiff silty clay lies underneath the soft clay layer. The groundwater level is located at the ground surface (Fig. 5). The undrained shear strength determined from the cone penetration tests varies from 15 to 35 kPa. The moisture content of the soil is generally close to or above the liquid limit. The void ratio is generally within the range of 0.8-1.5. A detailed description of the project has been reported elsewhere by Chu and Yan (2005).

As the undrained shear strength of the dredged soft soil is close to zero, the vacuum preloading method was selected to improve the soil characteristics. The required preloading pressure to attain the desired settlement with acceptable long-term settlement was 140 kPa. With an 80kPa vacuum pressure, an additional fill surcharge preloading was used to improve the shear strength of the soil. Among three embankment subsections, only Sections II and III will be analysed in this paper. The vertical cross-section and the locations of field

instrumentation for Sections II and III are presented in Fig. 6, including the multi-level gauges, settlement gauges, piezometers and inclinometers. PVDs (100 mm × 3 mm) with 20m length were installed at 1m spacing in a square pattern. A 0.3m thick sand blanket was placed to serve as a platform for the PVD installation rig. It was required to place horizontal perforated pipes in the sand platform to apply and distribute vacuum pressure under the membrane system. The modified Cam-Clay parameters for all clay layers??are shown in Table 2.

Three-dimensional finite element analysis

As the aspect ratio of Section III footprint (width/length) was close to 1 (15/25), a three dimensional (3D) finite element analysis was considered essential?? (Rujikiatkamjorn et al. 2008). A finite element software (ABAQUS v.6.7.1) was used to simulate the 3D multi-drain analysis (SIMULIA, 2009). More than 90000 C3D8RP solid elements were used during the analysis (8-node tri-linear displacement and pore pressure) (Fig. 7). A total of 350 individual PVDs were represented and to simulate the vacuum boundary, the pore pressure was set along drain length to the amount of suction generated by the applied vacuum. A 150mm x 200mm rectangular smear zone was simulated around the drain elements. This equivalent area of the rectangular smear zone equals to that of a circular 200mm diameter smear zone (i.e. 2 times the equivalent diameter of the mandrel). The well resistance was neglected due to the very high discharge capacity of the drain, i.e. q_w>120m^3/year (Indraratna and Redana 2000).

Two-dimensional finite element analysis

The equivalent plane strain parameters determined from Equations (15)-(21) with vacuum application was adopted and the same section described earlier under 3D DEM was analysed under the plane strain condition. These 2D (plane strain) results will be used in

comparison with 3D analyses. The 2D finite element mesh consisted of 14400 C2D8RP solid elements (8-node displacement and pore pressure) (Fig. 8). Considering the embankment symmetry, only one-half of the embankment was simulated. The vacuum pressure was specified by the negative pore pressure boundaries along the length of the drains.

NUMERICAL RESULTS AND THEIR COMPARISON WITH FIELD DATA

In this section, the predictions based on the equivalent 2D plane strain and 3D finite element analyses are compared with the field data including settlement, lateral displacement and excess pore pressure. Figure 9 shows a comparison between the predicted and measured field settlements at the embankment centreline with the loading sequence. As expected, the predicted settlements agree with the field data. The average volume of the extracted water per drain from the soil was $1.6m^3$/drain (3D analysis). This value depends not only on the discharge capacity of the drain, but also on the soil properties in the smear and undisturbed zones.

The comparison of predicted excess pore water pressure variation with time, at a depth of 5.5m and 0.25 m away from the embankment centreline is illustrated in Fig. 10. The surcharge loading effect is shown by the increase in time-dependent pore pressure (indicated by arrows in Fig. 10). It can be seen that the reduction of pore pressures obtained from 2D analysis is more than that obtained from 3D FEM analysis during the initial two months. As expected, the pore pressure reduction becomes constant (-80 kPa) after about 120 days. Figure 11 illustrates the comparison between the measured and predicted lateral movements at the toe of the embankment after 5.5 months. The negative lateral displacement denotes an inward soil movement towards the centreline of the embankment. Again, the predictions from 2D and 3D agree well with the measured data.

In general, the results obtained from the actual 3D and equivalent 2D approach based on the permeability conversion proposed by Indraratna et al. (2005a) are only slightly different to each other. In this method, the entire consolidation curve obtained from the equivalent 2D condition is almost the same as that of the 3D condition, thereby reducing the differences of pore pressure and lateral displacement predictions between the two analyses. In this context, this study shows that the equivalent plane strain analysis can be applied with confidence to obtain an acceptable accuracy, rather than having to always depend on a more cumbersome three-dimensional analysis.

CONCLUSIONS

A system of vertical drains combined with vacuum and surcharge preloading is an effective method for accelerating soil consolidation. In this study, an analytical model for consolidation via spectral method incorporating vacuum preloading as well as smear and well resistance was presented to consider the effect of the change in soil properties in a multi-layer soil. The versatility of the spectral model was demonstrated to accurately predict the soil behaviour subjected to vacuum pressure in both large-scale test and trial embankments at the Suvarnabhumi Airport. This case history analysis showed that the accurate prediction of complex vacuum assisted preloading can be captured to consider the actual multi-layer soil.

A 2D and 3D finite element code (ABAQUS) was employed to analyse the behaviour of a trial embankment subjected to vacuum preloading at Tianjin Port, China. A conversion procedure based on the transformation of permeability was introduced to compare the relative differences between the axisymmetric (3D) and equivalent plane strain (2D) conditions. The field behaviour as well as the model predictions indicate that the efficiency of vertical drains depends on the magnitude and distribution of vacuum pressure. In general, results obtained from the equivalent 2D approach were only slightly different to the 3D analysis, unless

embankment aspect ratio approached unity. This shows that the equivalent plane strain analysis can be applied with confidence for acceptable accuracy, rather than having to always rely on a sophisticated and cumbersome three-dimensional analysis. To estimate the drain spacing, convenient design charts were developed in lieu of time-consuming trial and error methods. These design charts permit rapid manual calculations without the aid of a computer, and they are of great benefit to the practicing engineer.

ACKNOWLEDGEMENT

APPENDIX A: DESIGN CHARTS FOR DETERMINING DRAIN SPACING

Rujikiatkamjorn and Indraratna (2008) proposed design charts eliminating cumbersome iteration procedures using the equivalent drain diameter as an independent variable to obtain the relevant drain spacing. The design steps are summarised below:

1. Use the available soil profiles, in-situ test measurements and laboratory data to obtain the relevant soil properties, hence, determine the appropriate installation depth (l), and the desired consolidation time (t);

2. Assume the required degree of consolidation U_t for surcharge fill alone;

3. For vacuum pressure application, specify the mean suction, p_0, required total design stress $\Delta\sigma$, and the surcharge fill pressure, Δp and then determine the required degree of consolidation from $U_{t,vac} = \left(\Delta\sigma/\left(p_0 + \Delta p\right)\right)*U_t$

4. Use c_v, t and l, to determine u^* using Fig. 12 or from,

$$u^* = \sum_{m=1}^{\infty} \frac{8}{(2m+1)^2 \pi^2} \exp\left(-\left(\frac{2m+1}{2}\right)^2 \pi^2 T_v\right) \qquad (22)$$

5. Determine the available size of the prefabricated vertical drains (circular or wick shape) and then compute the equivalent drain diameter (for wick drains), d_w from $d_w = 2(a+b)/\pi$;

6. Find T_h' from:

$$T_h' = c_h t \big/ d_w^2 \qquad (23)$$

7. Calculate $\gamma = -\dfrac{8T_h'}{\ln\left(\dfrac{1-U_t}{u^*}\right)}$ for surcharge fill only (no vacuum), $\qquad (24)$

or $\gamma = -8T_h' \big/ \ln\left(\dfrac{1-U_{t,vac}}{u^*}\right)$ for vacuum pressure plus surcharge fill $\qquad (25)$

8. Establish the diameter and permeability of the smear zone;

9. Determine ξ using Fig. 13 or from the equation:

$$\xi = \left(\frac{k_h}{k_s} - 1\right) \ln(s) \tag{26}$$

10. Calculate n from $n = \exp(\alpha \ln \gamma + \beta)$; $\qquad$ (27)

where, $\quad \alpha = 0.3938 - 9.505 \times 10^{-4} \xi^{1.5} + 0.03714 \xi^{0.5}$ $\qquad$ (28a)

and $\quad \beta = 0.4203 + 1.456 \times 10^{-3} \xi^2 - 0.5233 \xi^{0.5}$; $\qquad$ (28b)

11. Calculate the influence zone ($d_e = n d_w$);

12. Choose the drain pattern and determine the spacing of drain (d) from either $d = d_e/1.05$ (triangular grid) or $d = d_e/1.128$ (square grid).

Worked-out Example

The required soil parameters for the project are assumed to be: U_t = 90%, l = 24m, d_w = 34 mm (circular drain: Mebra-MCD34), c_h = 2.5 m^2/year, c_v = 1.0m^2/year, k_h/k_s = 5, s = 3, Maximum Design Surcharge, $\Delta\sigma$ = 120 kPa, surcharge fill pressure, Δp = 60 kPa, vacuum pressure, p_0 = -60kPa (suction). Well resistance is neglected. Calculate the drain spacing (d), for (a) t = 1.0 year; (b) t = 9 months; and (c) how the drain spacing can be altered with an increased vacuum pressure up to 90 kPa over 9 months.

Solution:

Part (a) t = 1.0 year

1. $T_v = 1.0 \times 1/24^2 = 0.002$; $U_{t,vac} = (120/(60+60)) * 0.9 = 0.9$

2. Calculate $u*$ using Equation 22 or from Fig. 12, hence, $u* = 0.95$

3. $T_h' = c_h t/d_w^2 = 2.5 \times 1.0/0.034^2 = 2163$

4. $$\gamma = -\frac{8T_h'}{\ln\left(\dfrac{1-U_{t,vac}}{u*}\right)} = -\frac{8 \times 2163}{\ln\left(\dfrac{1-0.9}{0.95}\right)} = 7686$$

5. From Fig. 13 or using Equation (26), $\xi = 4.39$

6. Using Equations (28a & 28b), determine $\alpha = 0.463$ and $\beta = -0.649$.

7. From Equation (27), $n = \exp(\alpha \ln \gamma + \beta) = \exp(0.463 \times \ln 7686 - 0.649) = 33$

8. Calculate d_e from, $d_e = n\, d_w = 33 \times 0.034 = 1.122$ m

9. Drain spacing = 1.1 m for triangular (1.122/1.05) or 1.0 m for square grid (1.122/1.128), respectively.

The above calculations confirm that the design spacing of 1m×1m used at Ballina Bypass. Australia can be justified for similar soil properties.

Part (b) $t = 0.75$ years (9 months)

1. $T_v = 1.0 \times 0.75 / 24^2 = 0.001$; $U_{t,vac} = (120/(60+60)) * 0.9 = 0.9$

2. Calculate $u*$ using Equation 22 or from Fig. 12; hence, $u* = 0.96$

3. $T_h' = c_h t / d_w^2 = 2.5 \times 0.75 / 0.034^2 = 1622$

4. $$\gamma = -\frac{8T_h'}{\ln\left(\dfrac{1-U_{t,vac}}{u*}\right)} = -\frac{8 \times 1622}{\ln\left(\dfrac{1-0.9}{0.96}\right)} = 5737$$

5. Using Fig. 13 or from Equation (26), $\xi = 4.39$

6. From Equations (28a and 28b), find $\alpha = 0.463$ and $\beta = -0.649$.

7. From Equation (27), $n = \exp(\alpha \ln \gamma + \beta) = \exp(0.463 \times \ln 5737 - 0.649) = 29$

8. Calculate d_e from $d_e = n\, d_w = 29 \times 0.034 = 0.986$ m

9. Drain spacing = 0.95m for triangular grid (i.e. 0.986/1.05) or 0.90m for square grid (i.e. 0.986/1.128).

Part (c): Vacuum pressure increased up to 90 kPa over 9 months. Revised Drain Spacing?

1. $T_v = 1 \times 0.75 / 24^2 = 0.001$; $U_{t,vac} = (120/(90+60)) * 0.9 = 0.72$

2. Calculate $u*$ using Equation 22 or Fig. 12, Hence, $u* = 0.96$

3. $T_h' = c_h t / d_w^2 = 2.5 \times 0.75 / 0.034^2 = 1622$

4. $\gamma = -\dfrac{8 T_h'}{\ln\left(\dfrac{1 - U_{t,vac}}{u*}\right)} = -\dfrac{8 \times 1622}{\ln\left(\dfrac{1 - 0.72}{0.96}\right)} = 10531$

5. Use Fig. 13 or Equation (26), $\xi = 4.39$

6. Using Equations (28a and 28b), find $\alpha = 0.463$ and $\beta = -0.649$.

7. From Equation (27), $n = \exp(\alpha \ln \gamma + \beta) = \exp(0.463 \times \ln 10531 - 0.649) = 38$

8. Calculate d_e from $d_e = n\, d_w = 38 \times 0.034 = 1.29$ m

9. Drain spacing = 1.23m for triangular pattern (i.e. 1.29/1.05) or 1.14m for square grid (i.e.1.29/1.128).

This demonstrates that increased vacuum pressure allows the drain spacing to be increased. This should also reduce the risk of smear overlapping and achieve reduced drain costs.

REFERENCES

Bergado, D.T, Chai, J.C, and Balasubramaniam, A.S (1998). PVD improvement of soft Bangkok clay using combined vacuum and reduced sand embankment preloading, Geotechnical Engineering Journal, 29 (1) 95-122.

Bergado, D.T., Balasubramanian, A.S., Fannin, R.J., Holtz, R.D., (2002). Prefabricated vertical drain (PVD) in soft Bangkok clay: a case of NBIA Project. Canadian Geotechnical Journal 39 (2), 304–315.

Chai, J. C., Shen, S. L., Miura, N. and Bergado, D. T. (2001) Simple method of modeling PVD improved subsoil. Journal of Geotechnical and Geoenvironmental Engineering, ASCE, 127 (11) 965-972.

Chai, J. C., Hong, Z.-S., and Shen, S.-L. (2010). Vacuum-drain method induced pressure distribution and ground deformation, Geotextiles and Geomemberanes, 28, pp. 525–535.

Chu, J., and Yan, S.W. (2005). Application of vacuum preloading method in soil improvement. Ground Improvement-Case Histories, Indraratna, B. & Chu, J. (Eds.), Elsevier, 91-118.

Chu, J. Yan, S.W. and Zheng, Y.R. (2006). Three soil improvement methods and their applications to road construction. Ground Improvement, 10 (3), 103- 112.

Chu, J., Yan, S.W. and Yang, H. (2000), Soil improvement by the vacuum preloading method for an oil storage station, Geotechnique 50 (6) pp. 625–632.

Hansbo, S. (1981). Consolidation of fine-grained soils by prefabricated drains and lime column installation. Proceedings of 10th International Conference on Soil Mechanics and Foundation Engineering, Balkema (Rotterdam) 3: 677-682.

Hird, C. C., Pyrah, I. C., and Russell, D. (1992). Finite element modelling of vertical drains beneath embankments on soft ground. Geotechnique, London, 42(3), 499–511.

Indraratna, B., and Redana, I.W. (2000). Numerical modeling of vertical drains with smear and well resistance installed in soft clay. Canadian Geotechnical Journal, 37: 133-145.

Indraratna, B., Bamunawita, C. and Khabbaz, H (2004). Numerical Modelling of Vacuum Preloading & Field Applications, Canadian Geotechnical Journal, Vol. 41, pp. 1098-1110.

Indraratna, B., Rujikiatkamjorn C., and Sathananthan, I. (2005a). Analytical and numerical solutions for a single vertical drain including the effects of vacuum preloading. Canadian Geotechinical Journal, 42, 994-1014.

Indraratna, B., Rujikiatkamjorn C., Balasubramaniam, A. S. and Wijeyakulasuriya, V. (2005b). Predictions and observations of soft clay foundations stabilized with geosynthetic drains and vacuum surcharge. Ground Improvement – Case Histories Book (Volume 3), Edited by Indraratna, B. and Chu, J., Elsevier, London, pp. 199-230.

Leong E.C., Soemitro R., and Rahardjo H. (2000). Soil Improvement by surcharge and vacuum preloading, Geotechnique 50(5): 601 – 605.

Mohamedelhassan, E., and Shang, J.Q. (2002). Vacuum and surcharge combined one-dimensional consolidation of clay soils. Can. Geotech. J. 39, 1126-1138.

Rujikiatkamjorn C. and Indraratna, B. (2009). Design procedure for vertical drains considering a linear variation of lateral permeability within the smear zone. Canadian Geotechnical Journal 46(3), 270-280.

Rujikiatkamjorn C., Indraratna, B. and Chu, J. (2008). 2D and 3D Numerical Modeling of Combined Surcharge and Vacuum Preloading with Vertical Drains. International Journal of Geomechanics, ASCE, 8(2), 144-156.

SIMULIA (2009). ABAQUS/Standard User's Manual, Published by HKS Inc.

Saowapakpiboon, J., Bergado, D.T., Youwai, S., Chai, J.C., Wanthong, P. and Voottipruex, P. (2010). Measured and predicted performance of prefabricated vertical drains (PVDs) with and without vacuum preloading, Geotextile and Geomembranes, 28(1), 1-11.

Seah, T.H. (2006). Design and construction of ground improvement works at Suvarnabhumi Airport. Geot. Eng, J. of Southeast Asian Geot. Society, 37, 171-188.

Shang, J.Q., Tang, M., and Miao, Z. (1998). Vacuum preloading consolidation of reclaimed land: a case study. Canadian Geotechnical Journal, 35, 740-749.

Tran, T.A. and Mitachi, T. (2008). Equivalent plane strain modeling of vertical drains in soft ground under embankment combined with vacuum preloading. Computers and Geotechnics 35(5): 655-672.

Walker, R. (2006). Analytical solutions for modeling soft soilconsolidation by vertical drains. PhD thesis, University of Wollongong, NSW, Australia.

Walker, R. and Indraratna, B. (2006). Vertical Drain Consolidation with Parabolic Distribution of Permeability in Smear Zone. J. of Geotechnical & Geoenvironmental Engineering, ASCE, Vol. 132(7), 937-941.

Walker, R. and Indraratna, B. (2007). Vertical drain consolidation with overlapping smear zones. Geotechnique, Institution of Civil Engineers, UK, 57(5). pp. 463-467.

Walker, R. and Indraratna, B. (2009). Consolidation analysis of a stratified soil with vertical and horizontal drainage using the spectral method, Géotechnique, 59(1), 1-11.

List of Tables

List of Figures

Table 1 Soil parameters for the test embankments (After Walker and Indraratna 2009)

Depth (m)	λ	κ	ν	Γ	e_0	γ (kN/m³)	k_v (10⁻⁹ m/s)	k_h (10⁻⁹ m/s)	$k_v/\bar{k}_v$	$\eta/\bar{\eta}$	$m_v/\bar{m}_v$
0-2	0.3	0.03	0.3	2.3	1.8	16	15.1	30.1	2.36	2.36	0.37
2-8.5	0.7	0.08	0.3	5.1	2.8	15	6.4	12.7	1.00	1.00	1.00
8.5-10.5	0.5	0.05	0.25	4.4	2.4	15	3.0	6.0	0.47	0.47	0.34
10.5-13	0.3	0.03	0.25	3.0	1.8	16	1.3	2.6	0.20	0.20	0.25
13-15	0.1	0.01	0.25	1.6	1.2	18	0.3	0.6	0.05	0.05	0.09

Table 2. Soil parameters in 2D and 3D FEM analysis (After Rujikiatkamjorn et al. 2008)

Depth (m)	λ	κ	ν	Γ	e_0	γ kN/m³	k_v 10^{-10} m/s	$k_{h,ax}$ 10^{-10} m/s	$k_{s,ax}$ 10^{-10} m/s	$k_{h,ps}$ 10^{-10} m/s	$k_{s,ps}$ 10^{-10} m/s
0.0-3.5	0.12	0.03	0.3	1.4	1.1	18.3	6.67	20	6.67	5.91	1.46
3.5-8.5	0.14	0.03	0.25	1.6	1.0	18.8	13.3	40	13.3	11.8	2.92
8.5-16.0	0.20	0.04	0.3	2.3	1.4	17.5	6.67	20	6.67	5.91	1.46
16.0-20.0	0.10	0.02	0.27	1.4	0.9	18.5	1.67	5	1.67	1.48	0.365

Note: κ Slope of consolidation curve for unloading stage

λ Slope of consolidation curve for loading stage after preconsolidation pressure

ν Poisson's ratio in terms of effective stress at in-situ effective stress

γ_w Unit weight of soil

OCR   Overconsolidation ratio
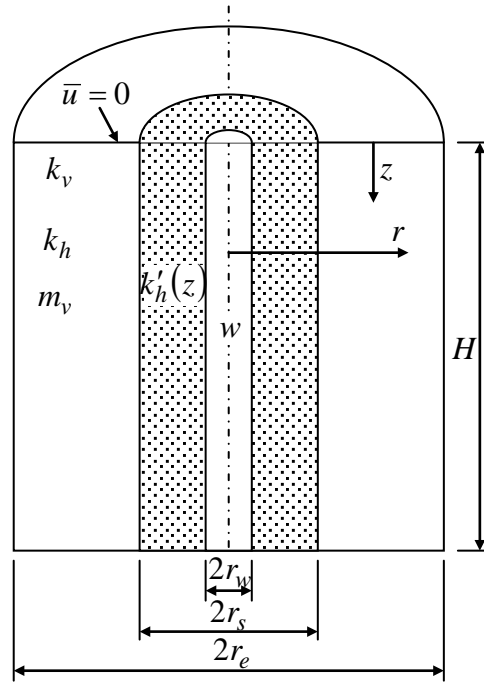
Fig. 1. Unit cell
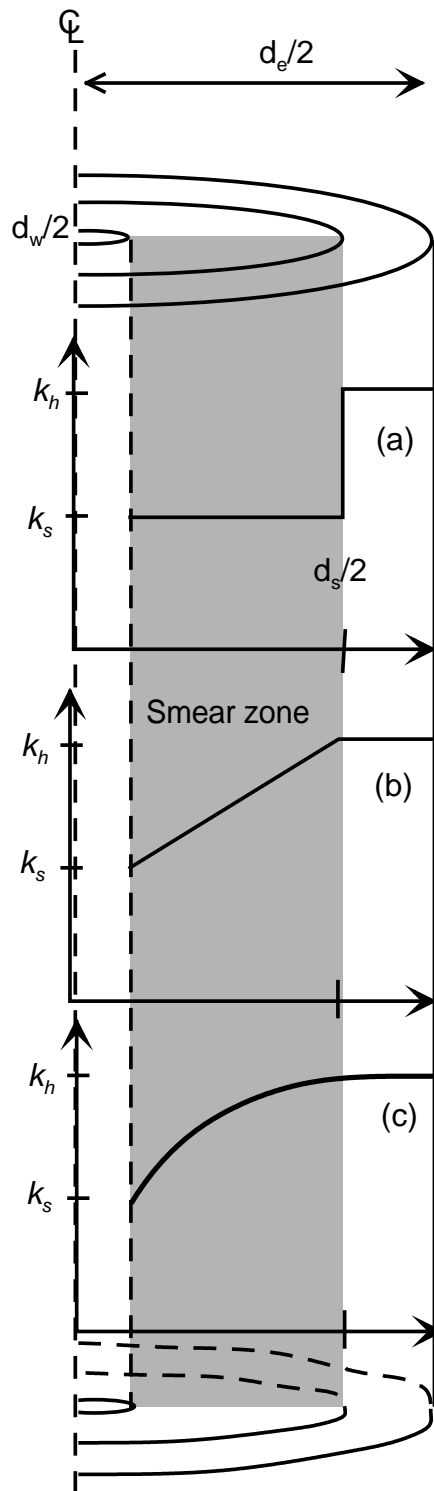
Fig. 2. Permeability distribution in smear zone (a) constant (b) linear and (c) parabolic
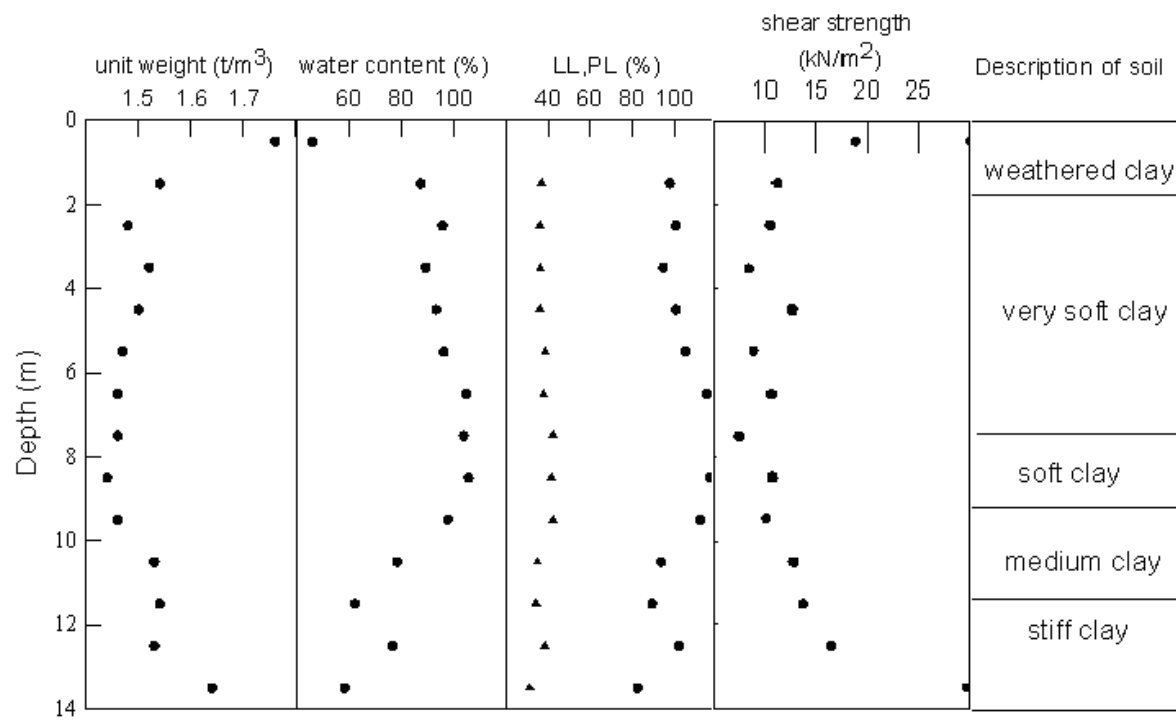
Fig. 3. Soil profile at the Suvarnabhumi Airport (After Indraratna et al. 2005b)
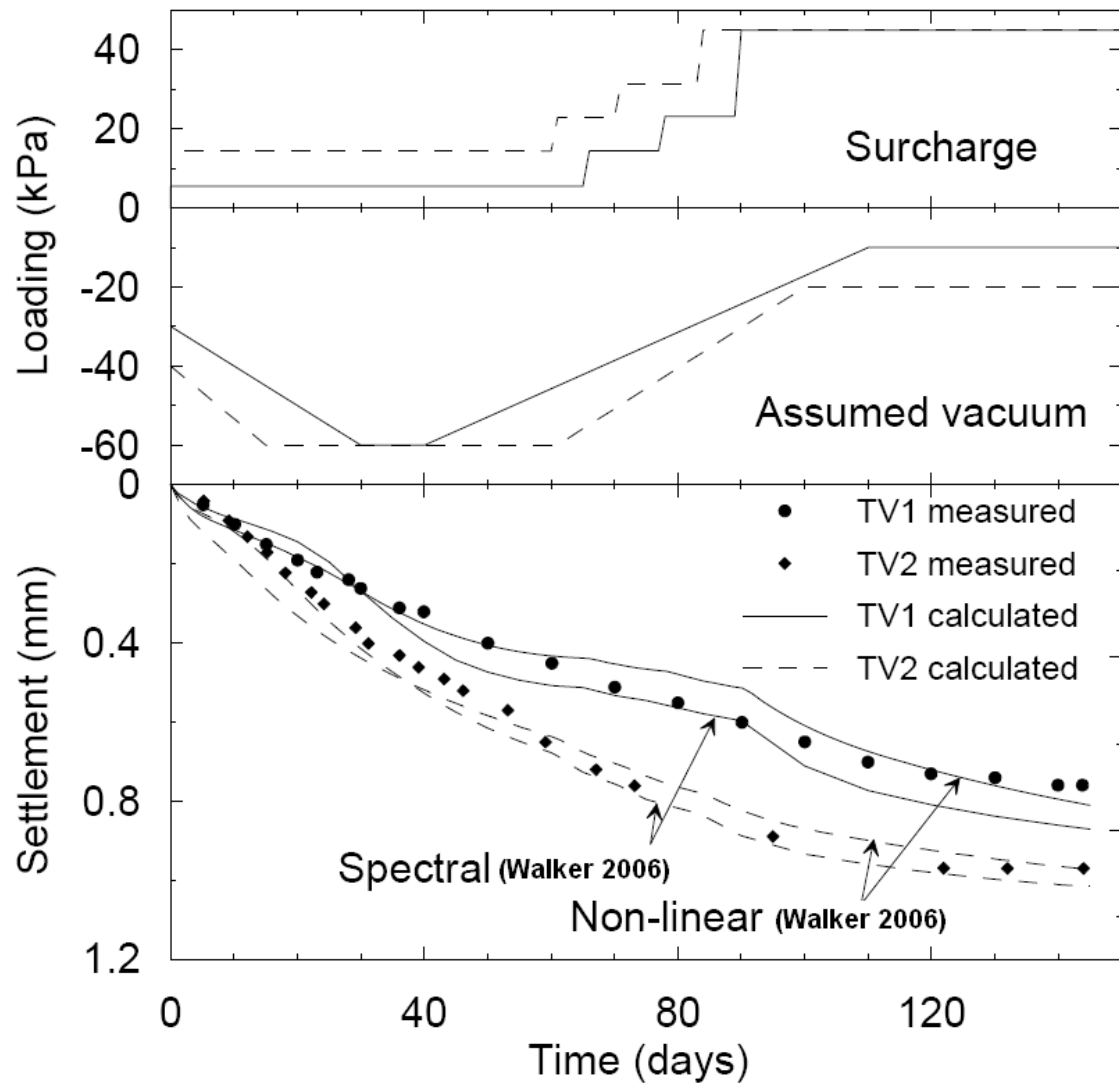
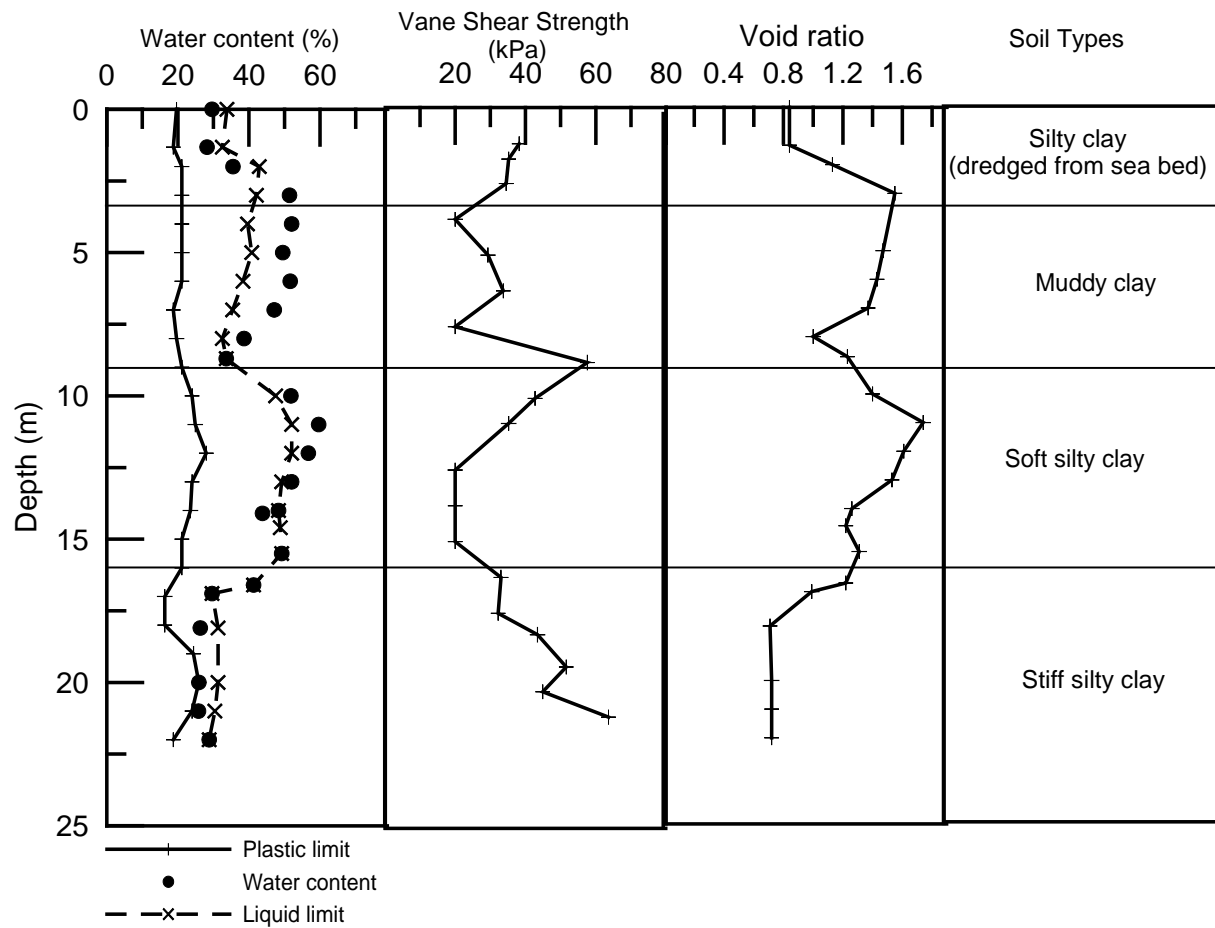Fig. 4. Measured and predicted settlement at Suvarnabhumi Airport (After Walker 2006)

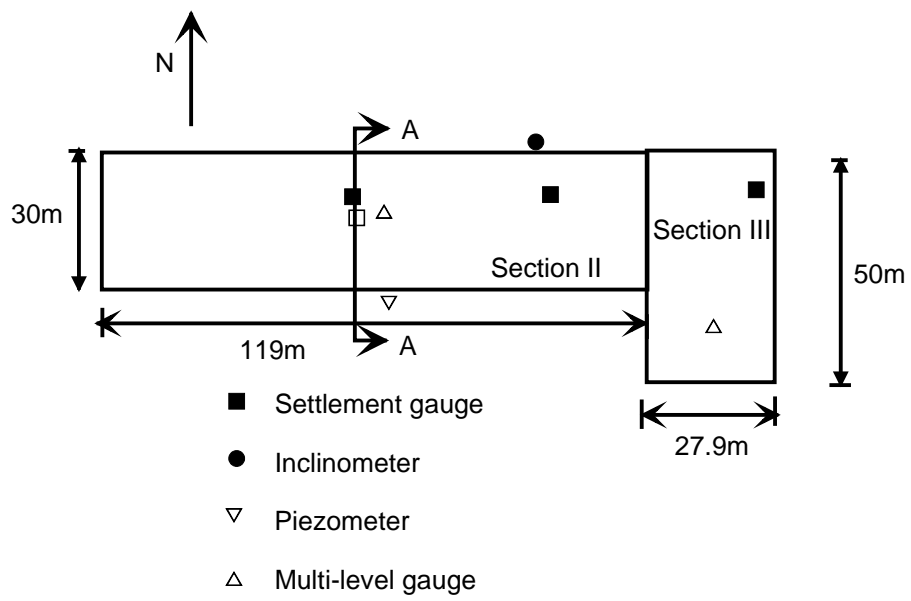Fig.5. Soil profiles at Tianjin Port (After Chu and Yan 2005)

Fig. 6. Embankment plan view with field instrumentation(After Chu and Yan 2005)
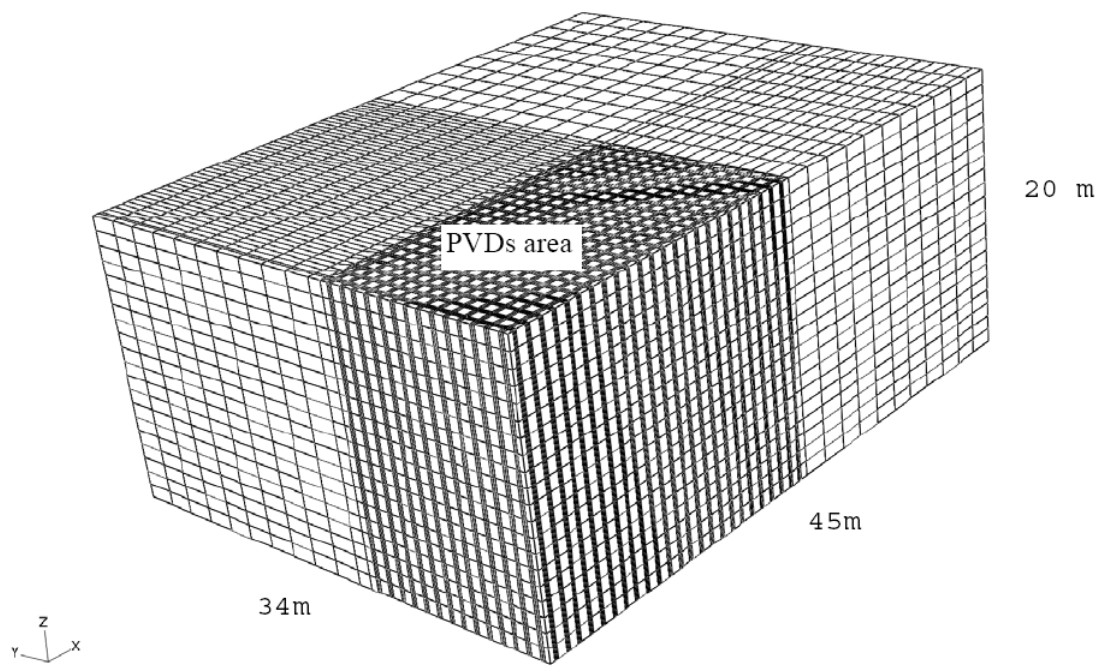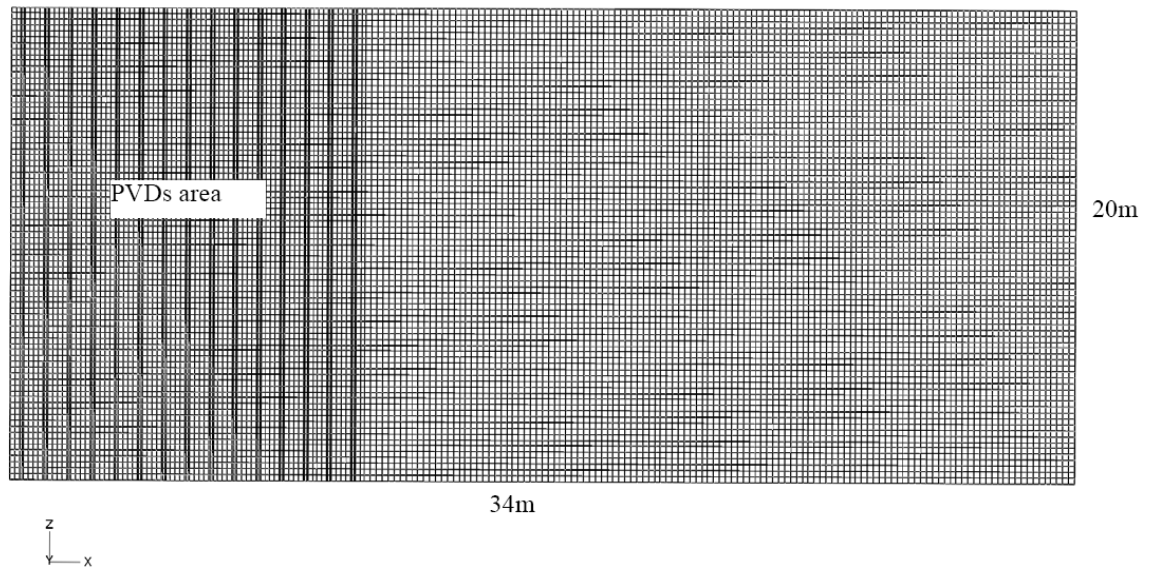
Fig. 7. 3D finite element mesh discretisation

Fig. 8. 2D finite element mesh discretisation
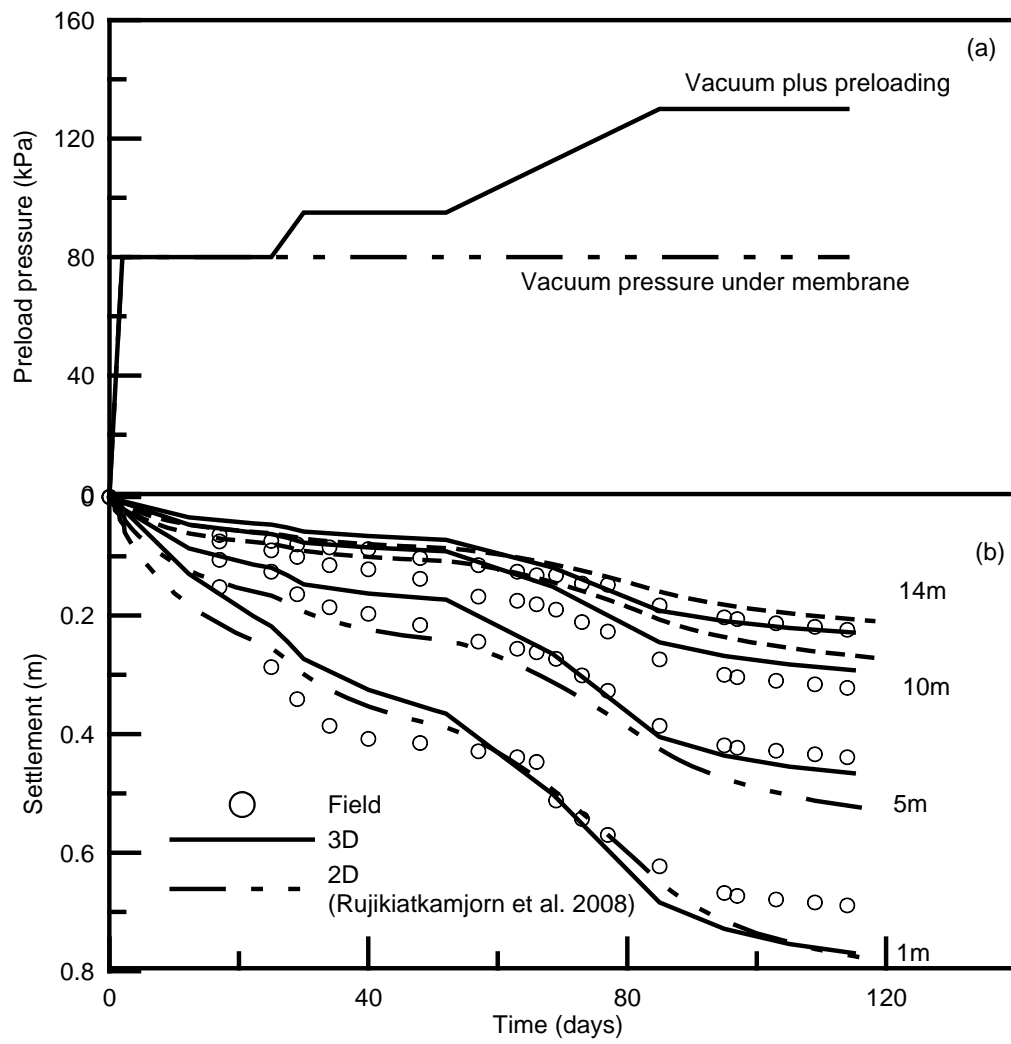
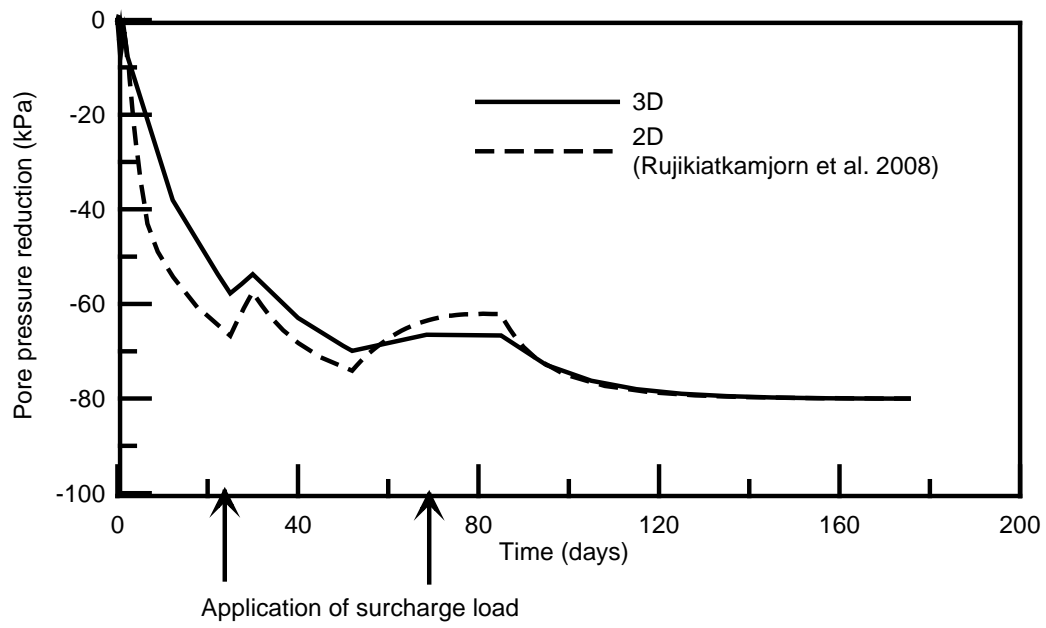Fig.9. (a) Loading history and (b) Consolidation settlements

Fig. 10 Pore pressure variation (Section III) at 0.25m away from the embankment centerline at 5.5m depth (arrows indicate times when surcharge loads were applied)
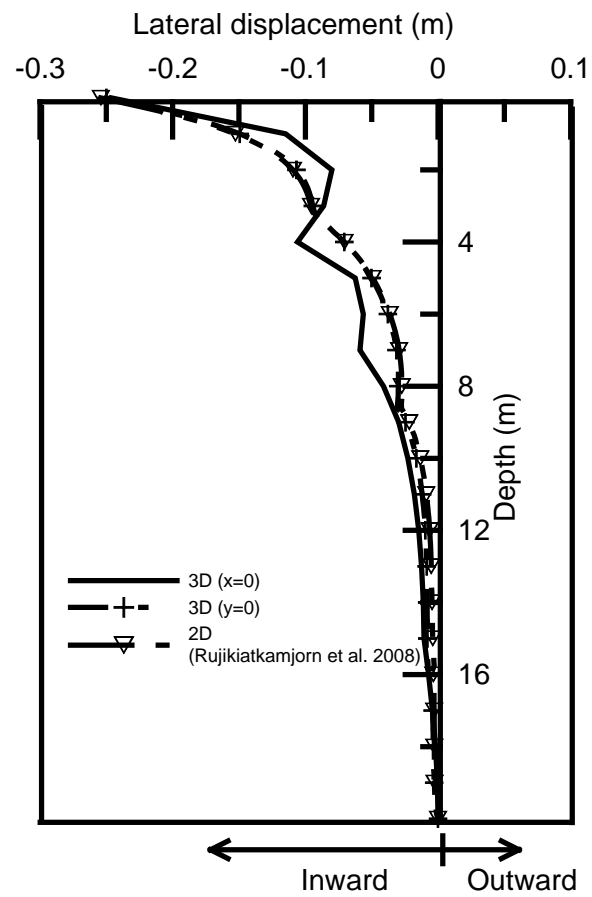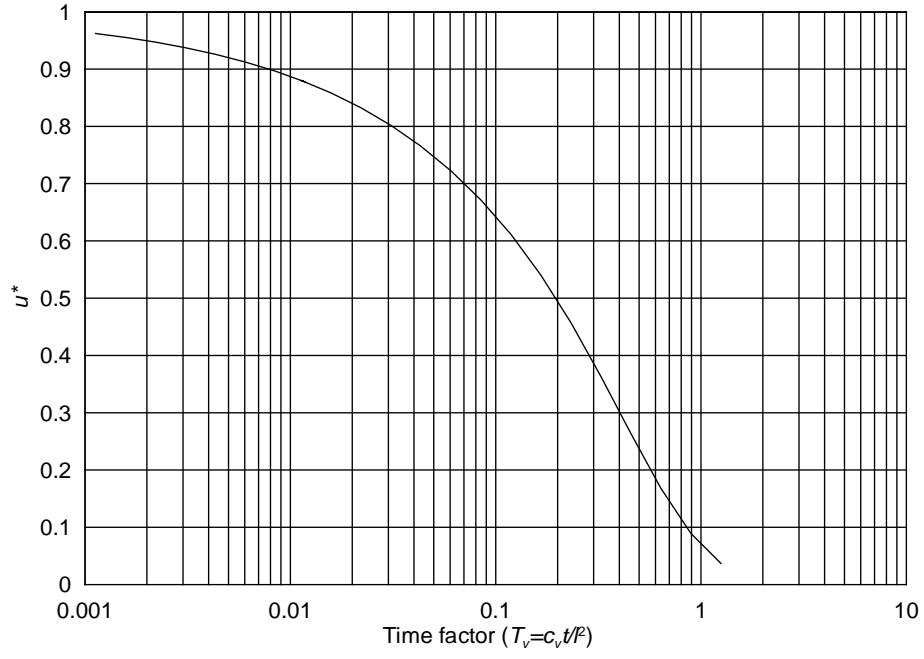
Fig. 11 Lateral displacements at embankment toe at 180th day

Fig. 12. Relationship between T_v and u^* (Rujikiatkamjorn and Indraratna 2009)
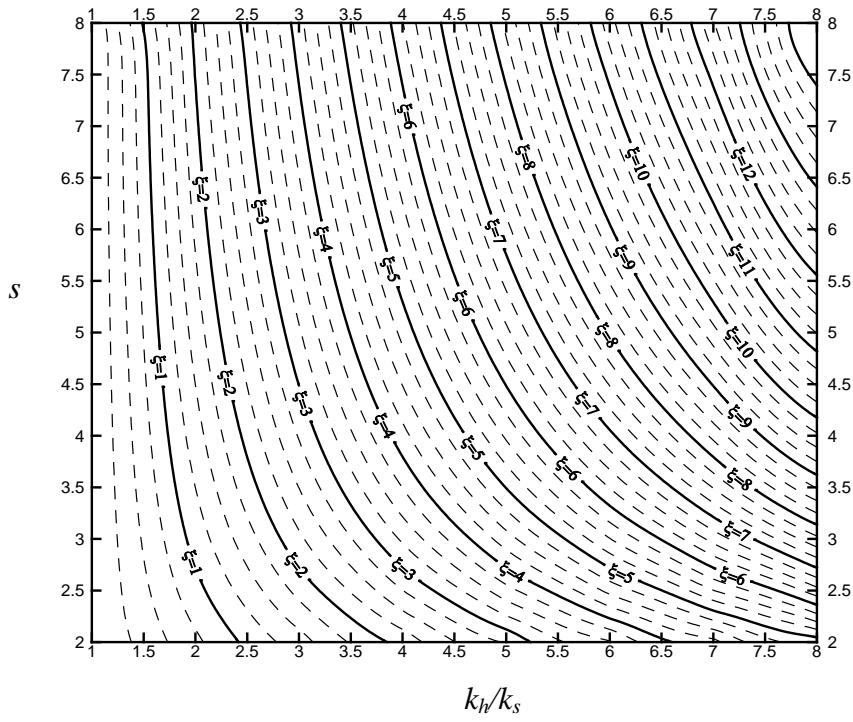

Fig. 13. Contour plot of ξ based on Equation (19) (Rujikiatkamjorn and Indraratna 2009)